Geophysical Research Letters

RESEARCH LETTER
10.1029/2021GL095195

Key Points:

- The February–March 2021 paroxysms at Etna produced the most intense deflation of the volcanic edifice in the last two decades
- The different phases of inflation preceding the paroxysms were accompanied by a deepening over time of the internal pressure sources
- The volcanic pressure source ascended rapidly two months before the first 2021 paroxysm, associated with an increase of volcanic gas flux

Supporting Information:

Supporting Information may be found in the online version of this article.

Correspondence to:

V. Bruno,
valentina.bruno@ingv.it

Citation:

Bruno, V., Aloisi, M., Gambino, S., Mattia, M., Ferlito, C., & Rossi, M. (2022). The most intense deflation of the last two decades at Mt. Etna: The 2019–2021 evolution of ground deformation and modeled pressure sources. *Geophysical Research Letters*, *49*, e2021GL095195. https://doi.org/10.1029/2021GL095195

Received 15 JUL 2021
Accepted 4 MAR 2022

Author Contributions:

Conceptualization: V. Bruno, M. Aloisi, M. Mattia, C. Ferlito
Data curation: V. Bruno, S. Gambino, M. Mattia
Formal analysis: V. Bruno, M. Aloisi, S. Gambino, M. Rossi
Investigation: V. Bruno
Methodology: V. Bruno, M. Aloisi, S. Gambino, M. Mattia, C. Ferlito
Resources: M. Rossi
Software: M. Rossi
Supervision: V. Bruno
Validation: V. Bruno, M. Aloisi

The Most Intense Deflation of the Last Two Decades at Mt. Etna: The 2019–2021 Evolution of Ground Deformation and Modeled Pressure Sources

V. Bruno[1], M. Aloisi[1], S. Gambino[1], M. Mattia[1], C. Ferlito[2], and M. Rossi[1]

[1]Istituto Nazionale di Geofisica e Vulcanologia, Osservatorio Etneo, Catania, Italy, [2]Dipartimento di Scienze Biologiche, Geologiche e Ambientali, Università degli Studi di Catania, Catania, Italy

Abstract We analyze Global Navigation Satellite System (GNSS) and tilt data from the permanent monitoring networks of Etna volcano starting just after the 24 December 2018 eruption to an unusual two-month period of deflation in February–March, 2021, which coincided with the occurrence of 17 lava fountain episodes. Based on changes in slope in the GNSS displacement time series, we divide the period starting 7 months after the eruption into five phases, spanning the continued inflation of the edifice punctuated by short periods of effusive and strombolian activity (four phases) and a 2-month phase of intensive deflation. Our model indicates a progressive deepening of the internal pressure sources followed by a fast ascending source starting two-months before the first 2021 paroxysms. We explain these results in light of a recent volcanological model on the nature and behavior of magma ascending through the Etnean feeding system.

Plain Language Summary On 16 February 2021, an eruptive phase characterized by 17 paroxysms from the Southeast Crater began at Etna volcano, producing km-high volcanic plumes and large tephra fallouts, causing hazard to air traffic and impacting inhabited areas. The paroxysms caused the most intense deflation of the volcanic edifice in the last two decades. We model both the inflation phases preceding the paroxysms and the period of deflation to investigate the internal pressure sources. Data suggest that the volcanic pressure source deepens progressively, during the recharging phases, and ascends only 2 months before the start of the paroxysms. A complex interaction between the high amounts of volatile elements dissolved in the molten rock and the arrival of new melt intrusions from depth allowed us to explain this singular behavior.

1. Introduction

From 16 February to the end of March 2021, the eruptive activity of Etna volcano (Italy) was characterized by a sequence of 17 lava fountain episodes from the South East Crater (SEC), which produced one of the most intense deflations (Figure 1) observed over the past two decades (e.g., Aloisi, Mattia, Ferlito, et al., 2011; Bruno et al., 2012; Bruno et al., 2016) and involved the entire volcanic edifice. All the lava fountains had similar characteristics. They started with strombolian activity that rapidly increased and shifted to lava fountains in a few hours. The paroxysmal phases were accompanied by lava flows and copious tephra emissions. The eruption columns rose several kilometers above the summit area, producing the fall of ash and lapilli in the urbanized areas around the volcano. The tephra fallout caused major problems to infrastructure and considerable hazard for aviation, with temporary closures of the Catania International Airport.

In this paper, we analyze the ground deformations preceding and accompanying the 17 lava fountains using Global Navigation Satellite System (GNSS) and tilt data. We start our analysis seven months after the end of the 24 December 2018 eruption (Mattia et al., 2020), that induced an exceptionally large southeastward displacement of the eastern flank of the volcano and the reactivation of its tectonic structures (Monaco et al., 2021). The GNSS southeastward velocities of the unstable eastern flank increased drastically to values of about 300 mm/yr soon after the intrusion (Mattia et al., 2020), compared to values of about 30 mm/yr over the preeruptive period.

After the December 2018 eruption, the volcanic edifice started a new period of continued inflation that was measured by the GNSS monitoring network (Figure 1a). The inflation was briefly interrupted during May–June 2019, July 2019, December 2019, April–May 2020 and December 2020. In particular, between 30 May and 5 June 2019, effusive activity was observed at the New SEC (NSEC, see inset in Figure 1b). In the course of July 2019, NSEC was characterized by effusive and strong strombolian activities. During December 2019, strong

Visualization: V. Bruno, M. Aloisi, S. Gambino
Writing – original draft: V. Bruno, M. Aloisi, S. Gambino, M. Mattia, C. Ferlito

strombolian activity occurred at SEC, NSEC and Voragine Crater. On 19 April 2020, a modest lava fountain episode was observed at NSEC together with strong strombolian activity between April and May 2020. Moreover, from November 2020, strombolian activity restarted at the SEC with intensity and frequency varying over time, until December 2020, when two paroxysmal episodes occurred on 13 and 21 December. From the end of 2020, the two craters NSEC and SEC were morpho-structurally indistinguishable and hereinafter we will assign to them the acronym SEC. From January 2021, sustained strombolian activity at SEC continued until 16 February when a rhythmic sequence of 17 paroxysms began.

We model the different pressure sources that produced the measured deformations on Etna volcano between 2019 and 2021. We discuss the progressive deepening of the internal pressure sources followed by a fast ascending source starting two-months before the first 2021 paroxysms with reference to a recent model published by Ferlito (2018) on the nature and behavior of magma rising through the Etnean feeding system.

2. Methods

Data from GNSS and tilt permanent networks (see Text S1 in the Supporting Information S1 for network descriptions and data processing) were used together to investigate medium and short-term pressure sources at different spatial scales. GNSS has a homogeneous coverage over the volcanic edifice, enabling it to detect the medium-term inflation/deflation phases. The tilt network, on the other hand, can detect the effect of small and short-term phenomena such as the lava fountains with a greater precision. We modeled the GNSS ground deformation patterns for each different phase preceding the February–March 2021 paroxysms. Velocity fields (Figures 2a–2e) show how ground deformations evolved in the different sectors of Mt. Etna, driven by the pressure sources that we modeled (Figure 3). Moreover, the deflation occurring during the 17 paroxysms (Figure 2e) was modeled using both GNSS and tilt data. Finally, the first lava fountain of the eruptive cycle (Figure 2f) was modeled using exclusively tilt data.

3. Data Analysis and Modeling

3.1. GNSS Data

After the end of the December 2018 eruption, we observed an overall trend of inflation at the volcano edifice, evidenced by a positive trend in the areal variation of a triangle of the three GNSS stations, EINT-EMEG-EDAM (Figure 1c). It was interrupted by brief periods of areal contractions, closely correlated with episodic eruptive activity at the summit craters. We started our analysis from the second half of 2019 because a strong eastern flank sliding, begun during the December 2018 eruption (Mattia et al., 2020), was still ongoing during the first half of 2019. Subsequently, from August 2019, we identified five sub-intervals (Figures 1c and 1d). In particular, the time series follow a near-linear trend, interrupted by five changes in slope, as evidenced in Figure 1d, in which the radial components to the summit craters of the stations set on different flanks of the volcano are shown. During time periods characterized by a near-linear trend, we can infer that a stationary pressure source is active. Therefore, we can describe the analyzed period through five temporal sub-intervals, considering them as "snapshots" that represent the kinematic time evolution of the plumbing system before and during the 2021 eruptive activity. The first four phases of inflation preceded the February–March 2021 paroxysms (Figures 2a–2d). The fifth phase was the intense deflation recorded during the paroxysms (Figure 2e). The first inflation phase (01 August–31 December 2019) was characterized by a radial deformation pattern which was still strongly influenced by the instability of the eastern flank of Mt. Etna, induced by the December 2018 eruption (Figure 2a). The second phase (01 January–31 July 2020) was characterized by a general decrease in velocities (Figure 2b). The velocity pattern was not radial. Indeed, the velocities of summit GNSS stations (EPDN, ECNE, EPLU and ECPN) were all southeastern oriented and the vector of ECPN rotated counterclockwise with respect to the first phase, suggesting a westward shift of the inflating source. In the third phase (01 August–24 November 2020) the velocities of all the GNSS stations started increasing in the radial direction (Figure 2c). The fourth period (12 January–15 February 2021) was the last phase of the inflation that preceded the beginning of lava fountains. It was characterized by a significant increase of velocities (Figure 2d) although, due to the shortness of this analyzed temporal interval, the GNSS velocities have large uncertainties that make them suitable only for qualitative analysis. Finally, the fifth phase (16 February–24 March 2021) was characterized by an unusual deflation pattern involving the entire

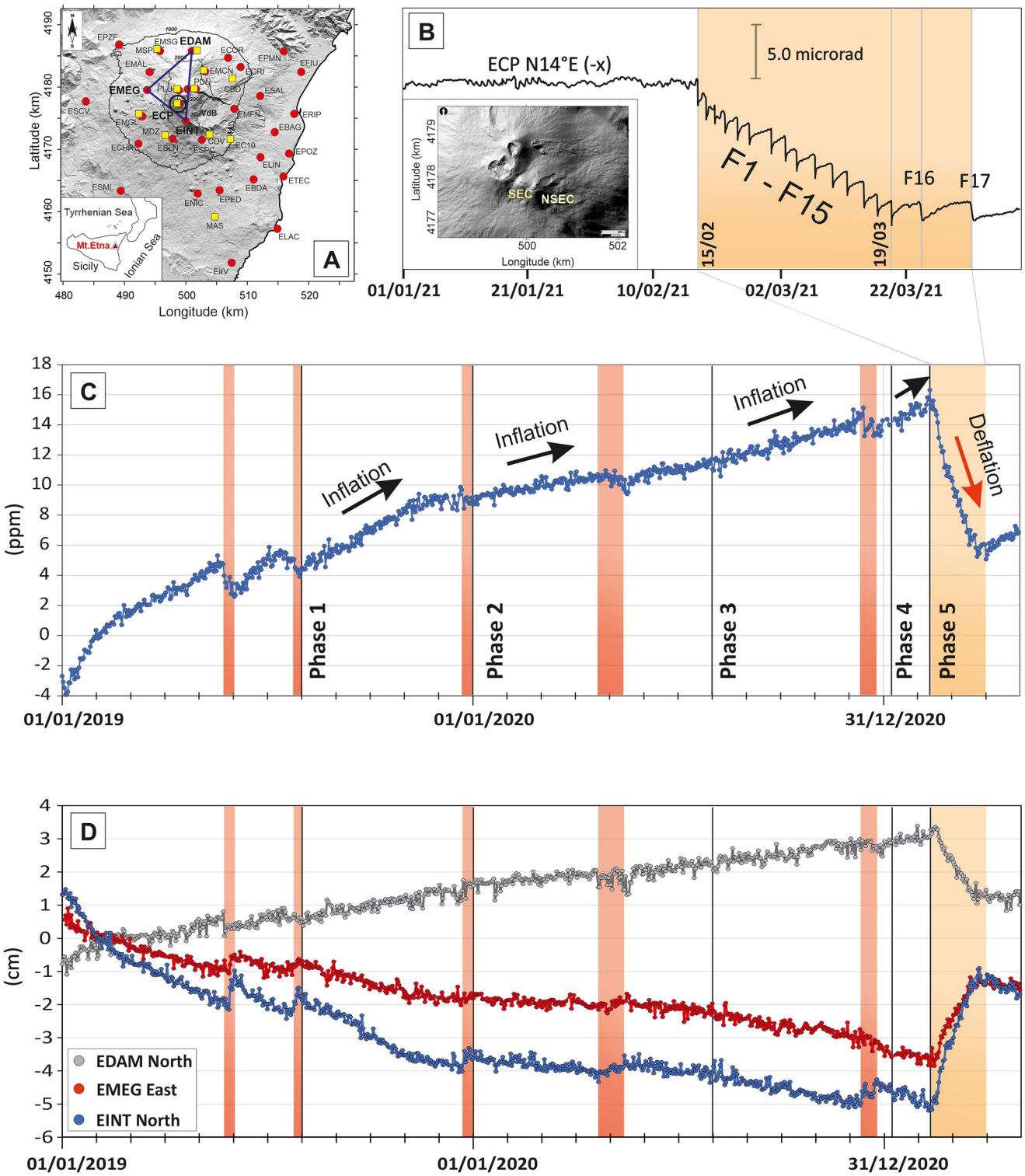

Figure 1.

volcanic edifice including the eastern flank, that is usually affected by a near continuous southeastward sliding toward the sea (e.g., Aloisi, Mattia, Monaco, & Pulvirenti, 2011; Bruno et al., 2012; Bruno et al., 2017; Mattia et al., 2015). We also show the measured displacements path for the five phases in Figure S1 in the Supporting Information S1. It evidences the major changes in directions during the second phase, particularly in the summit

area, and the continuous southeastward displacements in the eastern flank. Furthermore, it highlights how the deflation phase is quite pronounced.

3.2. Tilt Data

During each paroxysm, the tilt stations recorded signal variations characterized by sharp increases, with changes no higher than 1.0 μrad, except for ECP station, positioned close to SEC, that showed larger amplitudes (2–3 μrad) (Figure 1b). Signals were very similar for each episode (Figure 1b). Tilt trends changed starting from the first episode (16 February 2021), evidencing a general lowering toward the summit area and suggesting a deflation phase that ended with the fifteenth paroxysm (19 March 2021). The last two fountains started and ended gradually, recording smaller variations with respect to previous episodes.

3.3. Modeling

We modeled the five subphases and the 16 February 2021 lava fountain by an analytical inversion of GNSS and tilt data using the software developed by Cannavò (2019). For the inflation phases (Figures 2a–2d), we did not use the GNSS stations located on the eastern flank of the volcano because it is affected by an almost constant ESE-ward motion whose origin is still controversial and not directly related to the magmatic process of uprising (e.g., Aloisi, Mattia, Monaco, & Pulvirenti, 2011; Mattia et al., 2015). The first and the second phase were characterized by a non-uniform deformation pattern, probably due to a combined action of a magmatic source and secondary dislocations along tectonic structures. We imaged the two phases using an arbitrarily oriented, finite, prolate and spheroidal cavity (Yang et al., 1988). Regarding the radial deformation pattern characterizing the third and fifth phases, we used the spherical source model of McTigue (1987). We verified that the McTigue (1987) source is sufficient to obtain a good fit for the fourth phase, although we consider this phase more qualitative due to the high errors of the velocity field. We maintain that vertical variations for the first four phases were affected by local effects or by dislocations along not well-known seismic structures and, therefore, not easily modeled. In particular, their magnitude was lower than the recording uncertainty (about 0.01 m; Aloisi et al., 2003; Bonaccorso et al., 2002). Furthermore, the stations located near seismic structures showed negative vertical variations during the inflation. Exclusively during the deflation phase, vertical variations were greater than the uncertainty of measurement and showed negative values (Figure S2 in the Supporting Information S1). Final optimal solutions for each phase are reported in Figure 3 and Table 1.

4. Results and Discussion

A key issue on active volcanoes is the evolution of the magma pressure sources over time. In this manuscript, we analyze ground deformations data that cover a period longer than two years, from 2019 to 2021. An inflation of the volcanic edifice is clearly noticeable until the first half of February 2021. It produced an areal dilatation of about 20 ppm at an intermediate altitude triangle (Figure 1c). Such an inflation, associated with an overpressure occurring within the magmatic feeding system, is traditionally interpreted as an intrusion of batches of molten rock. Whereas, we apply the paradigm published by Ferlito (2018), trying to provide a more exhaustive interpretation. According to Ferlito (2018), the magma rising through the Etnean feeding system should not be considered merely as molten rock with a relatively scarce amount of volatile elements dissolved in it. Rather, it can be interpreted as a flux of fluid continuously moving upwards, in which two vertical portions can be recognized. Below is a solution made up of ~70% in volume by a continuum gas phase (mostly H_2O) at

Figure 1. (a) Maps of Etna volcano with the Global Navigation Satellite System (GNSS) (red circles) and tilt (yellow squares) permanent networks; the blue triangle highlights the area whose variation is shown in Figure (c), while the black circle indicates the ECP tilt station. VdB indicates the Valle del Bove area. The inset at the left bottom shows the location of Mt. Etna in southern Italy; (b) Tilt recorded on the N14°E component of ECP station during the fountain sequence tilt series: F1-F15 shows changes associated with the first 15 fountains also characterized by a general lowering trend ending with the last two episodes (F16 and F17). The inset at the left bottom shows the summit crater of Mt. Etna (De Beni et al., 2015). SEC, South East Crater; NSEC, New SEC; (c) Daily variation of the area recorded at an intermediate altitude triangle (EDAM-EMEG-EINT) indicated by the blue triangle in Figure (a). Positive variations indicate inflations, while negative variations are measured during deflations of the volcanic edifice, due to volcanic activity; (d) N-S daily components of the EINT and EDAM GNSS stations (blue and gray circles, respectively), on the southern and northern flanks of Mt. Etna, respectively. E-W daily component of the EMEG station (red circles), located on the western flank. Red rectangles indicate short and episodic interruptions of the inflation due to summit eruptive activity. The orange rectangles highlight the deflation produced by the 17 lava fountains. The vertical black lines indicate the start of each phase characterized by a different ground deformation pattern, recognized on the basis of the changes in the slope of the time series. Black arrows indicate inflation, while the red arrow indicates the deflation of volcanic edifice.

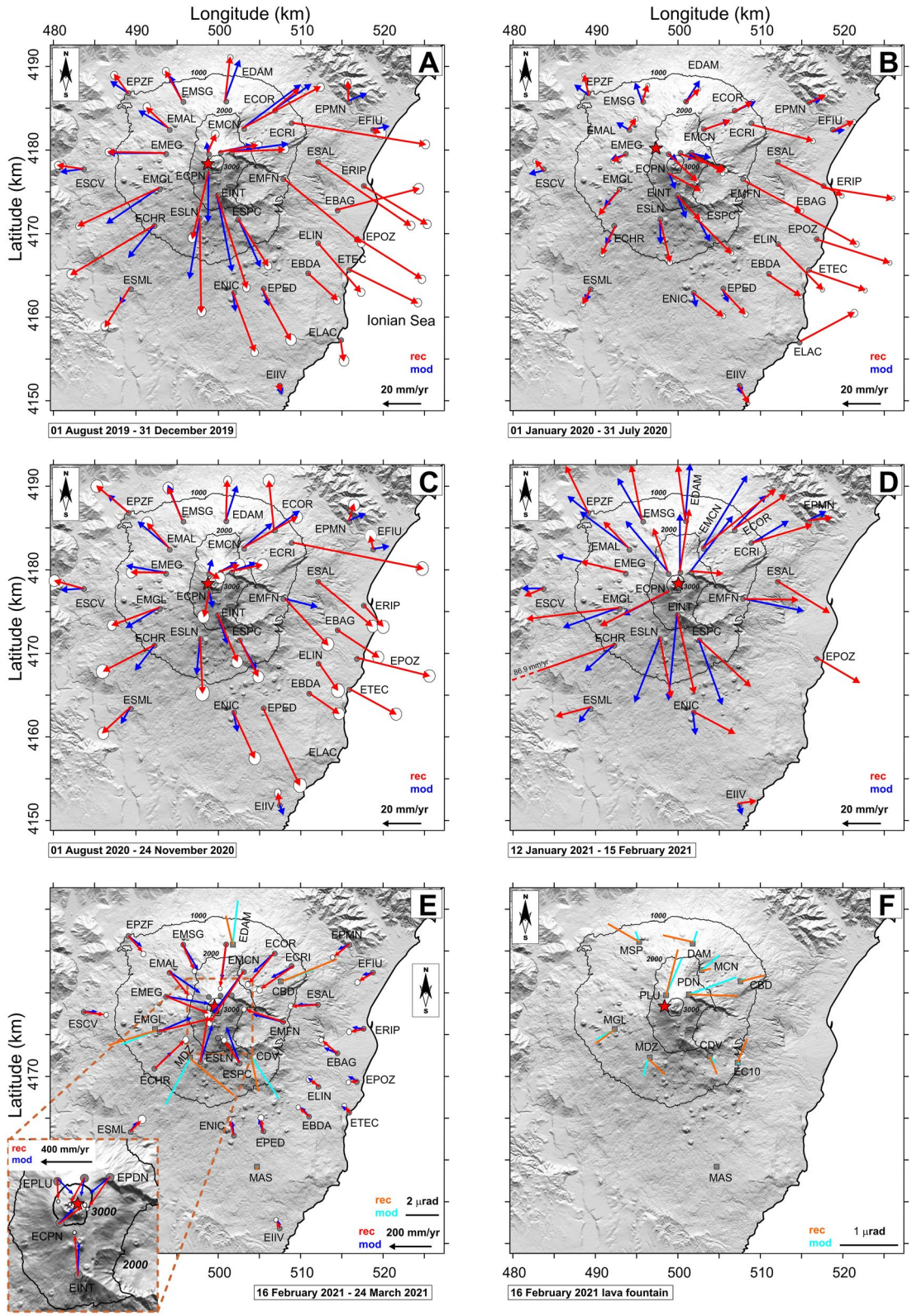

Figure 2. (a, b, c, d, and e) Observed Global Navigation Satellite System (GNSS) horizontal velocities (red arrows) with 95% confidence ellipses and modeled velocities (blue arrows) for each of the five phases indicated in Figures 1c and 1d. Error ellipses are not reported in Panel (d) as the analyzed time interval is very short and computed velocities are affected by large errors; in (e) recorded (orange lines) and modeled (light blue lines) tilt vectors are also shown. In (f) tilt vectors for the 16 February 2021 lava fountain are reported. The red stars in each phase represent the locations of the modeled pressure sources.

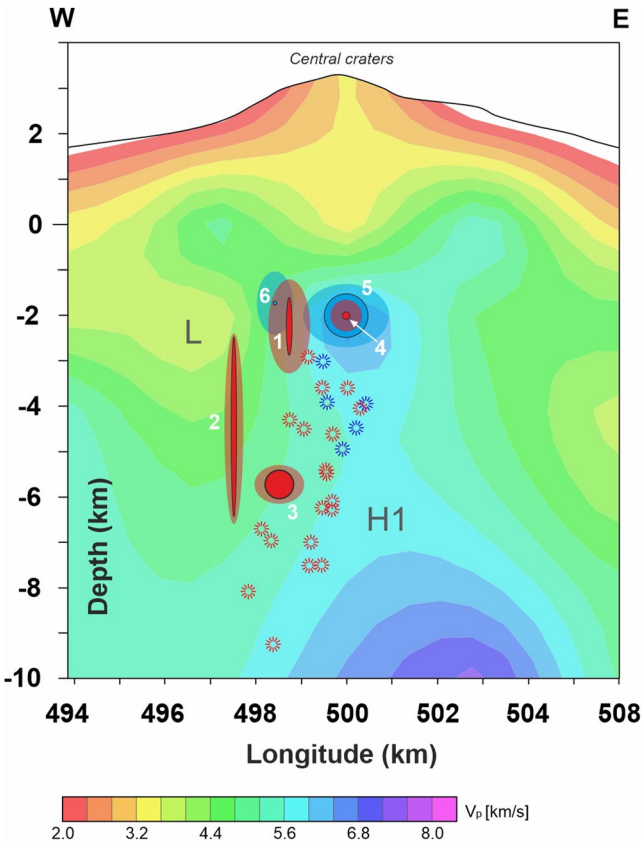

Figure 3. W-E section of Mt. Etna passing through the Central craters and showing the position of the modeled sources for each of the five deformation phases of the volcanic edifice (indicated with progressive numbers from 1 to 5, inflation in red and deflation in blue), for the 16 February 2021 lava fountain (indicated with number 6) and inferred by several authors since 1992 (represented by asterisks). Blurred areas around each pressure source represent the related uncertainties. In the background, vp velocities are also reported (redrawn from Aloisi et al., 2002).

a supercritical state (density 360 kg/m^3) and ~30% in volume by basaltic components dissolved in it, named water melt solution (WMS); the overall density is low (ca.1140 kg/m^3). At the top of the WMS, the continuous loss of gas, characterizing the persistent activity of the Etnean volcano, will leave a highly dense (2,800 kg/m^3) basaltic melt, defined as a continuous melt phase (CMP). The CMP has a low viscosity to permit the passage of the gas bubbles coming from the WMS. The transition between the WMS and the CMP can be erratic within the plumbing system. In this new paradigm of magma, the eruptions can be considered as being due to a significant pressure increase within the WMS in the deep plumbing system, which cannot be kept confined by the weight of the overlying basaltic melt (CMP). Therefore, the source of the overpressure, that causes deformations, can be associated with variations of the stationary fluid flux. Variations can be related to an increase or decrease in the flux discharge rate, or alternatively, as due to an increase in viscosity of the CMP that, decreasing its permeability, hinders the upward migration of the gas bubbles. The occurrence of such conditions will end up with an overpressure of the entire feeding system, which might trigger an eruptive event. Theoretically, we can recognize two distinct patterns in the deformation sources. A first one might be produced by a source in which the increased overpressure of the gas-rich WMS pushes against the country rock. When the gas is released, the deformation could be near completely retrieved. On the contrary, a pressure source associated with a permanent deformation can be interpreted as a batch of CMP intruding within the uppermost section of the feeding system. Such accumulations could occur along horizontally elongated discontinuities, leading to the formation of sills, similarly to what must have happened during the early phase of Etna's evolution (Trifoglietto eruptive center). Indeed, several subvolcanic bodies are fairly well visible in the Valle del Bove area, embedded within the rock successions (Ferlito, 1994).

With these theoretical arguments in mind, we can interpret the results of our analysis. During the second half of 2019 (first phase), we observed the action of a prolate source of inflation. It can be interpreted as an increased overpressure in the WMS, located at a depth of −2.1 Km (b.s.l.). This increase might be due to a decreased permeability of the system to the gas release, related to a viscosity increase in the uppermost section of the feeding system. A further increase in WMS overpressure could be deemed responsible for the deepening of the deformation source during 2020 (Phase 2). We modeled a prolate source located at about −4.4 km (b.s.l.). The deformation in Phase 3, during the last months of the 2020, which was produced by a deep (−5.7 km, b.s.l.) spherical source, indicates that, besides the WMS overpressure, there might be another component such as new melt intrusion coming from depth. The eruptive event of 13 December 2020 seems to change the conditions of the volcano that leaves the stationary regime state. A clear increase in SO_2 release has been observed, associated with that event (INGV, 2021), indicating that the overpressure accumulated in the previous phases began to be released. In the last inflation (Phase 4), that ended with the beginning of the paroxysms (the first on 16 February), the source became shallower (−2.0 Km, b.s.l.), probably due to an increase of overpressure in the WMS, which could be associated with an increase of the volcanic gas flux, as demonstrated by the high SO_2 release (INGV, 2021). The beginning of the paroxysms, on 16 February 2021, produced an intense and rapid deflation due to the gas release in WMS and melt release in the CMP, which reduced the previously accumulated overpressure. Similarly, we observed the sharp drop of the SO_2 plume flux down to background level (INGV, 2021). This fifth phase was imaged by a deflation source located at −2.0 km (b.s.l.). It can be considered as a near-perfect elastic response of the entire volcanic edifice. In fact, the eastern flank was also affected by the deflation process. This phase includes the most intense deflation on Mt. Etna over the last two decades. Its exceptional nature consists not only in the measured displacements, but in the short time period over which they occurred, namely a little more than a month, from 16 February to 24 March 2021. From 2004, we measured

Table 1
Model Parameters and Related Uncertainties (Standard Deviations of the Class of Solutions That Satisfy the Chi-Square Test for Our Degrees of Freedom Within the Significance Level of 5%)

Parameters	Phase 1	Phase 2	Phase 3	Phase 4	Phase 5	Lava fountain
Source	Yang et al. (1988)	Yang et al. (1988)	McTigue (1987)	McTigue (1987)	McTigue (1987)	McTigue (1987)
Data type	GNSS	GNSS	GNSS	GNSS	GNSS + Tilt	Tilt
X [m]	498797 ± 400	497508 ± 150	498478 ± 250	500150 ± 250	499936 ± 450	498284 ± 350
Y [m]	4179485 ± 500	4180706 ± 1300	4178846 ± 100	4178072 ± 250	4178562 ± 170	4178683 ± 150
Z [m]	−2193 ± 400	−4424 ± 120	−5747 ± 130	−2016 ± 250	−2010 ± 200	−1793 ± 650
a [m]	642 ± 85	1988 ± 900				
b/a	0.1 ± 0.1	0.03 ± 0.2				
θ [°]	32 ± 15	71 ± 5				
φ [°]	128 ± 35	288 ± 10				
ΔV [m^3]	+3.2 E+06 ± 3.8 E+05	+2.9 E+06 ± 1.0 E+05	+3.8 E+06 ± 2.5 E+06	+1.0 E+06 ± 1.2 E+06	−5.8 E+06 ± 1.0 E+05	−4.8 E+05 ± 2.0 E+03
Reduced chi-squared	0.70	0.59	0.28	0.13	0.73	0.10

Note. Reduced chi-square is obtained considering the a-posteriori standard deviations of 0.005 [m] and 0.010 [m] for the horizontal and vertical displacements and 1.0 [mrad] for the tilt components. Source depth refers to sea level. Coordinates are reported in UTM-WGS84.

different phases of deflation of the volcanic edifice associated with eruptions (as the 2004–2005, 2006 and 2008 eruptions, see Aloisi, Mattia, Ferlito, et al., 2011; Bruno et al., 2012) or eruptive episodes characterized by sequences of strombolian activity that eventually evolved into lava fountains (as the 2013 volcanic activity, see Bruno et al., 2016). Nevertheless, we have never measured before deflation phases with GNSS velocities that reached values of 275 mm/yr in the summit area and as much as 87 mm/yr at the peripheral stations (e.g., ESCV station, the westernmost point in the network, Figure 2e).

Finally, we also sought to model the position of the source generating the single lava fountain that occurred on 16 February ("F" in Figure 2 and "6" in Figure 3). We obtained a depth of about −1.8 km (b.s.l.) but this result was not very well constrained. In fact, variations were clearly visible exclusively on the clinometric signals. In any case, it is interesting to highlight that the depth levels activated by the fourth inflation phase pre-fountains (−2.0 km), by a single fountain (−1.8 km) and, finally, by the entire eruptive cycle (−2.0 km), are very similar. This shallow level of the plumbing system is compatible with one of the three volumes where De Gori et al. (2021) found a significant reduction of seismic wave velocity since 2019 (see also Bonaccorso et al., 2021).

Indeed, although we know that modeled pressurized cavities are just "mathematical artifacts" that mimic the strain/stress field of the physical deformation sources (Segall, 2019), our modeled volume variations well correspond with the location of the magma ascent paths found by tomographic studies (Figure 3; Aloisi et al., 2002). In particular, the pressure sources (1), (4), (5), and (6) are located where tomographic studies found a shallower magmatic storage, usually generating lava fountains (Bonaccorso et al., 2013). Moreover, our solutions (2) and (3) are located along the elongated storage zone corresponding to a low-velocity-domain (L) found on the western side of the high velocity body (H1; Figure 3). Many authors agree that this low-velocity zone includes both highly fractured rocks and paths for magma ascent and stationing. Therefore, we can hypothesize that our mathematical solutions correspond with "real" sources.

5. Conclusions

In this work, we have examined the ground deformations associated with the February–March 2021 Etnean paroxysms and the inflation of volcanic edifice preceding it, interpreting the dynamics of the sources of deformation as mostly due to overpressure increase or decrease in the gas-rich portion of the magma (WMS), within the feeding system (Ferlito, 2018). We have highlighted a progressive deepening over time of the pressure source during the inflation that preceded the lava fountains. In the last 20 years, there was a clear association of this phenomenon with strong explosive eruptions (Aloisi, Mattia, Ferlito, et al., 2011; Bonaccorso & Aloisi, 2021), particularly, before the 2011–2015 explosive activity and the explosive eruptions of 2001 and 2002.

The phase of paroxysms we have analyzed in this work produced the most intense deflation of the entire volcanic edifice observed through the GNSS permanent network in the last 20 years (e.g., Aloisi, Mattia, Ferlito, et al., 2011; Bruno et al., 2012, 2016). The deflation was so intense that it was even visible by the GNSS stations located along the coast line and on the lower eastern flank of the volcano that, typically, maintains an ESE-ward motion also during deflation phases (Bruno et al., 2012).

During the drafting of this paper, a new phase of lava fountains on Etna volcano resumed on 18 May 2021, after a short inflation phase following the February–

March 2021 paroxysms. This activity seems rather similar to the eruptive activity occurring between January and June 2000, consisting of 64 lava fountain episodes (Alparone et al., 2003). Both the 2000 and 2021 activity constitute an exceptional series of paroxysms within a short time in the known eruptive history of Etna (Andronico et al., 2021).

Data Availability Statement

The data reported in this paper can be freely downloaded in the FIGSHARE folder (https://doi.org/10.6084/m9.figshare.14986788.v1).

Acknowledgments
We thank the technicians of the Global Navigation Satellite System (Daniele Pellegrino, Mario Pulvirenti) and Tilt (Angelo Ferro, Giuseppe Laudani) permanent networks of the Istituto Nazionale di Geofisica e Vulcanologia, Osservatorio Etneo, who ensure the regular working of the stations. We thank Emanuela De Beni for the map of the summit area of Mount Etna. We are grateful to S. Conway for revising the text. Furthermore, we thank the Editor, Christian Huber, and the Reviewers, Maurizio Battaglia and an anonymous Reviewer, for their comments and constructive suggestions that led to the improvement of the original version of the manuscript. We also thank Flavio Cannavo' and Alessandro Bonaccorso for the useful discussions during the revision of the manuscript. Open Access Funding provided by Istituto Nazionale di Geofisica e Vulcanologia within the CRUI-CARE Agreement.

References

Aloisi, M., Bonaccorso, A., Gambino, S., Mattia, M., & Puglisi, G. (2003). Etna 2002 eruption imaged from continuous tilt and GPS data. *Geophysical Research Letters*, *30*(23), 2214. https://doi.org/10.1029/2003gl018896

Aloisi, M., Cocina, O., Neri, G., Orecchio, B., & Privitera, E. (2002). Seismic tomography of the crust underneath the Etna volcano, Sicily. *Physics of the Earth and Planetary Interiors*, *134*, 139–155. https://doi.org/10.1016/s0031-9201(02)00153-x

Aloisi, M., Mattia, M., Ferlito, C., Palano, M., Bruno, V., & Cannavò, F. (2011). Imaging the multi-level magma reservoir at Mt. Etna volcano (Italy). *Geophysical Research Letters*, *38*, L16306. https://doi.org/10.1029/2011GL048488

Aloisi, M., Mattia, M., Monaco, C., & Pulvirenti, F. (2011). Magma, faults, and gravitational loading at Mount Etna: The 2002–2003 eruptive period. *Journal of Geophysical Research*, *116*, B05203. https://doi.org/10.1029/2010JB007909

Alparone, S., Andronico, D., Lodato, L., & Sgroi, T. (2003). Relationship between tremor and volcanic activity during the Southeast Crater eruption on Mount Etna in early 2000. *Journal of Geophysical Research*, *108*(B5), 2241. https://doi.org/10.1029/2002JB001866

Andronico, D., Cannata, A., Di Grazia, G., & Ferrari, F. (2021). The 1986–2021 paroxysmal episodes at the summit craters of Mt. Etna: Insights into volcano dynamics and hazard. *Earth-Science Reviews*, *220*, 103686. https://doi.org/10.1016/j.earscirev.2021.103686

Bonaccorso, A., & Aloisi, M. (2021). Tracking magma storage: New perspectives from 40 Years (1980-2020) of ground deformation source modeling on Etna volcano. *Frontiers of Earth Science*, *9*, 638742. https://doi.org/10.3389/feart.2021.638742

Bonaccorso, A., Aloisi, M., & Mattia, M. (2002). Dike emplacement forerunning the Etna July 2001 eruption modeled through continuous tilt and GPS data. *Geophysical Research Letters*, *29*, 13. https://doi.org/10.1029/2001GL014397

Bonaccorso, A., Calvari, S., Currenti, G., Del Negro, C., Ganci, G., Linde, A., et al. (2013). From source to surface: Dynamics of Etna's lava fountains investigated by continuous strain, magnetic, ground and satellite thermal data. *Bulletin of Volcanology*, *75*. https://doi.org/10.1007/s00445-013-0690-9

Bonaccorso, A., Carleo, L., Currenti, G., & Sicali, A. (2021). Magma migration at shallower levels and lava fountains sequence as revealed by borehole dilatometers on Etna Volcano. *Frontiers of Earth Science*, *9*, ISSN=2296–6463. https://doi.org/10.3389/feart.2021.740505

Bruno, V., Ferlito, C., Mattia, M., Monaco, C., Rossi, M., & Scandura, D. (2016). Evidence of a shallow magma intrusion beneath the NE Rift system of Mt. Etna during 2013. *Terra Nova*, 1–363. https://doi.org/10.1111/ter.12228

Bruno, V., Mattia, M., Aloisi, M., Palano, M., Cannavò, F., & Holt, W. E. (2012). Ground deformations and volcanic processes as imaged by CGPS data at Mt. Etna (Italy) between 2003 and 2008. *Journal of Geophysical Research*, *117*, B07208. https://doi.org/10.1029/2011JB009114

Bruno, V., Mattia, M., Montgomery-Brown, E., Rossi, M., & Scandura, D. (2017). Inflation leading to a slow slip event and volcanic unrest at Mount Etna in 2016: Insights from CGPS data. *Geophysical Research Letters*, *44*, 12141–12149. https://doi.org/10.1002/2017GL075744

Cannavò, F. (2019). A new user-friendly tool for rapid modelling of ground deformation. *Computers & Geosciences*, *128*, 60–69. https://doi.org/10.1016/j.cageo.2019.04.002

De Beni, E., Behncke, B., Branca, S., Nicolosi, I., Carluccio, R., D'Ajello Caracciolo, F., & Chiappini, M. (2015). The continuing story of Etna's new Southeast Crater (2012–2014): Evolution and volume calculations based on field surveys and aerophotogrammetry. *Journal of Volcanology and Geothermal Research*, *303*, 175–186. https://doi.org/10.1016/j.jvolgeores.2015.07.021

De Gori, P., Giampiccolo, E., Cocina, O., Branca, S., Doglioni, C., & Chiarabba, C. (2021). Re-pressurized magma at Mt. Etna, Italy, may feed eruptions for years. *Commun Earth Environ*, *2*, 216. https://doi.org/10.1038/s43247-021-00282-9

Ferlito, C. (1994). Geologia e petrologia delle vulcaniti dell' area Sud-occidentale della Valle del Bove (Etna), Doctoral Dissertation, Università degli Studi di Catania.

Ferlito, C. (2018). Mount Etna volcano (Italy). Just a giant hot spring. *Earth-Science Reviews*, *177*, 14–23. https://doi.org/10.1016/j.earscirev.2017.10.004

INGV (Istituto Nazionale di geofisica e Vulcanologia). (2021). *Sezione di Catania e Palermo, Volcanic Monitoring Report, Etna Volcano, Italy, N. 14/2021*. Retrieved from https://www.ct.ingv.it/index.php/monitoraggio-e-sorveglianza/prodotti-del-monitoraggio/bollettini-settimanali-multidisciplinari

Mattia, M., Bruno, V., Caltabiano, T., Cannata, A., Cannavo, F., D'Alessandro, W., et al. (2015). A comprehensive interpretative model of slow slip events on Mt. Etna's eastern flank. *Geochemistry, Geophysics, Geosystems*, *16*, 635–658. https://doi.org/10.1002/2014GC005585

Mattia, M., Bruno, V., Montgomery-Brown, E., Patanè, D., Barberi, G., & Coltelli, M. (2020). Combined seismic and geodetic analysis before, during, and after the 2018 Mount Etna eruption. *Geochemistry, Geophysics, Geosystems*, *21*, e2020GC009218. https://doi.org/10.1029/2020GC009218

McTigue, D. F. (1987). Elastic stress and deformation near a finite spherical magma body: Resolution of the point source paradox. *Journal of Geophysical Research*, *92*, 12931–12940. https://doi.org/10.1029/JB092iB12p12931

Monaco, C., Barreca, G., Bella, D., Brighenti, F., Bruno, V., Carnemolla, F., et al. (2021). The seismogenic source of the 2018 December 26th earthquake (Mt. Etna, Italy): A shear zone in the unstable eastern flank of the volcano. *Journal of Geodynamics*, *143*, 101807. https://doi.org/10.1016/j.jog.2020.101807

Segall, P. (2019). Magma chambers: What we can, and cannot, learn from volcano geodesy. *Philosophical Transactions of the Royal Society A: Mathematical, Physical and Engineering Sciences*, *377*, 20180158. https://doi.org/10.1098/rsta.2018.0158

Yang, X. M., Davis, P. M., & Dieterich, J. H. (1988). Deformation from inflation of a dipping finite prolate spheroid in an elastic half-space as a model for volcanic stressing. *Journal of Geophysical Research*, *93*, 4249–4257. https://doi.org/10.1029/JB093iB05p04249

References From the Supporting Information

Ferro, A., Gambino, S., Panepinto, S., Falzone, G., Laudani, G., & Ducarme, B. (2011). High precision tilt observation at Mt. Etna Volcano, Italy. *Acta Geophysica*, *59*, 618–632. https://doi.org/10.2478/s11600-011-0003-7

Gambino, S., Aloisi, M., Di Grazia, G., Falzone, G., Ferro, A., & Laudani, G. (2019). Ground deformation detected by permanent tiltmeters on Mt. Etna summit: The August 23-26, 2018, strombolian and effusive activity case. *International Journal of Geophysics*. https://doi.org/10.1155/2019/1909087

Gambino, S., Falzone, G., Ferro, A., & Laudani, G. (2014). Volcanic processes detected by tiltmeters: A review of experience on Sicilian volcanoes. *Journal of Volcanology and Geothermal Research*, *271*, 43–54. https://doi.org/10.1016/j.jvolgeores.2013.11.007

Herring, T. A., Floyd, M. A., King, R. W., & McClusky, S. C. (2015). GLOBK: Global kalman filter VLBI and GPS analysis program. Reference manual. Mass. Inst. of Technol.

Herring, T. A., King, R. W., Floyd, M. A., & McClusky, S. C. (2018). GPS analysis at MIT. GAMIT reference manual. Mass. Inst. of Technol.

Palano, M., Rossi, M., Cannavò, F., Bruno, V., Aloisi, M., Pellegrino, D., et al. (2010). Etn@ref: A geodetic reference frame for Mt. Etna GPS networks. *Annals of Geophysics*, *53*(4), 49–57.